Radiative and correlation effects on the parity-nonconserving transition amplitude in heavy alkali-metal atoms

V. M. Shabaev,[1,2] I. I. Tupitsyn,[1] K. Pachucki,[3] G. Plunien,[4] and V. A. Yerokhin[1,5]
[1]*Department of Physics, St. Petersburg State University, Oulianovskaya 1, Petrodvorets, St. Petersburg 198504, Russia*
[2]*Max-Planck Institut für Physik Komplexer Systeme, Nöthnitzer Straße 38, D-01187 Dresden, Germany*
[3]*Institute of Theoretical Physics, Warsaw University, Hoża 69, 00-681 Warsaw, Poland*
[4]*Institut für Theoretische Physik, TU Dresden, Mommsenstraße 13, D-01062 Dresden, Germany*
[5]*Center for Advanced Studies, St. Petersburg State Polytechnical University, Politekhnicheskaya 29, St. Petersburg 195251, Russia*
(Received 3 October 2005; published 6 December 2005)

The complete gauge-invariant set of the one-loop QED corrections to the parity-nonconserving (PNC) amplitude in cesium and francium is evaluated to all orders in αZ using a local form of the Dirac-Fock potential. The calculations are performed in both length and velocity gauges for the absorbed photon and the total binding QED correction is found to be $-0.27(3)\%$ for Cs and $-0.28(5)\%$ for Fr. Moreover, a high-precision calculation of the electron-correlation and Breit-interaction effects on the $7s$-$8s$ PNC amplitude in francium using a large-scale configuration-interaction Dirac-Fock method is performed. The obtained results are employed to improve the theoretical predictions for the PNC transition amplitude in Cs and Fr. Using an average value from two most accurate measurements of the vector transition polarizability, the weak charge of ^{133}Cs is derived to amount to $Q_W=-72.65(29)_{\rm exp}(36)_{\rm theor}$. This value deviates by 1.1σ from the prediction of the standard model. The values of the $7s$-$8s$ PNC amplitude in ^{223}Fr and ^{210}Fr are obtained to be $-15.49(15)$ and $-14.16(14)$, respectively, in units of $i\times10^{-11}(-Q_W)/N$ a.u.

DOI: 10.1103/PhysRevA.72.062105 PACS number(s): 11.30.Er, 31.30.Jv, 32.80.Ys

I. INTRODUCTION

Measurements of the parity-nonconservation (PNC) effects in atoms provide sensitive tests of the standard model (SM) and impose constraints on physics beyond it [1,2]. The $6s$-$7s$ PNC amplitude in ^{133}Cs [3] remains one of the most effective tools for such investigations. The measurement of this amplitude to a 0.3% accuracy [4,5] has stimulated a reanalysis of the theoretical predictions given in Refs. [6–8]. First, it was found [9–13] that the role of the Breit interaction had been underestimated. Then, it was pointed out [14] that the QED corrections may be comparable with the Breit corrections. The numerical evaluation of the vacuum-polarization (VP) correction [15] led to a 0.4% increase of the $6s$-$7s$ PNC amplitude in ^{133}Cs, which resulted in a 2.2σ deviation of the weak charge of ^{133}Cs from the SM prediction. This has triggered a great interest to calculations of the complete one-loop QED corrections to the PNC amplitude.

While the VP contribution can easily be evaluated to a high accuracy within the Uehling approximation, the calculation of the self-energy (SE) contribution is a much more demanding problem (here and below we imply that the SE term embraces all one-loop vertex diagrams as well). In the plane wave approximation, that corresponds to zeroth order in αZ, it was derived in Refs. [16,17]. This correction, whose relative value is equal to $-\alpha/(2\pi)$, is commonly included in the definition of the nuclear weak charge. The αZ-dependent part of the SE correction to the PNC matrix element between s and p states was evaluated in Refs. [18,19]. These calculations, which are exact to first order in αZ and partially include higher-order binding effects, yield the binding SE correction of $-0.9(1)\%$ [18,20] and -0.85% [19]. The corresponding total binding QED correction was found to amount to -0.5% and -0.43%, respectively. Despite this restored agreement with SM, the status of the QED correction to PNC in ^{133}Cs could not be considered as resolved until a complete αZ dependence calculation of the SE correction to the $6s$-$7s$ transition amplitude is accomplished. This is due to the following reasons. First, in the case of cesium ($Z=55$) the parameter $\alpha Z\approx0.4$ is not small and, therefore, the higher-order corrections, which are beyond the $A(\alpha Z)\ln(\lambda_C/R_{\rm nuc})$ term [19], can be significant. Second, because the calculations [18–20] are performed for the PNC matrix element only, they do not include other SE diagrams which contribute to the $6s$-$7s$ transition amplitude. For instance, these calculations do not account for diagrams in which the virtual photon embraces both the weak interaction and the absorbed photon. Third, strictly speaking, the PNC matrix element between the states of different energies is not gauge invariant. Despite the gauge-dependent part is suppressed by the small energy difference [19], estimates of the uncertainty in the definition of the PNC diagrams may fail due to an unphysical origin of the gauge-dependent terms.

The first step towards a complete αZ-dependence calculation of the SE correction was done in Ref. [21], where the SE correction to the $2s$-$2p_{1/2}$ PNC matrix element in H-like ions was evaluated. This matrix element was chosen to deal with the simplified gauge-invariant amplitude. The results of that work agree with those of Refs. [18–20]. However, as was stressed there, no claims can be made about the applicability of these results to the $6s$-$7s$ PNC transition in neutral cesium.

Finally, the whole gauge-invariant set of the one-loop QED corrections to the $6s$-$7s$ PNC transition amplitude in cesium was evaluated in Ref. [22]. This calculation showed that the contributions of all SE diagrams are of the same order of magnitude (in both length and velocity gauges) and

the final result arises through a delicate cancellation of individual terms, none of which can be neglected. The binding SE correction was obtained to amount to −0.67(3)%, whereas the total binding QED correction is −0.27(3)%.

Recently, the one-loop radiative corrections to the 6*s*-7*s* PNC amplitude in cesium were reevaluated by a semiempirical method [23]. In addition to the radiative correction to the weak matrix element, this method accounts for the related corrections to the energy levels and to the electric dipole (E1) amplitude. Despite that it is intended to incorporate the radiative and correlation effects, it is unclear how the results obtained by this method are related to those derived in the framework of the rigorous QED approach. The total binding QED correction obtained in Ref. [23] amounts to −0.32(3)%.

In the present paper we describe in detail the complete αZ-dependence evaluation of the one-loop QED corrections to the PNC transition amplitude in alkali-metal atoms and present the corresponding numerical results for the 6*s*-7*s* PNC amplitude in cesium [22] and for the 7*s*-8*s* PNC amplitude in francium, which will be a subject of the PNC experiment, as proposed in Ref. [24]. Moreover, we perform a high-precision atomic structure calculation of the PNC transition amplitude in francium using a large-scale configuration-interaction Dirac-Fock (CI-DF) method and compare the results with those from Refs. [25,26]. The obtained contributions are combined with other terms in order to improve the theoretical predictions for the PNC transition amplitudes in Cs and Fr.

The relativistic units ($\hbar=c=1$) and the Heaviside charge unit [$\alpha=e^2/(4\pi), e<0$] are used throughout the paper.

II. QED CORRECTIONS

A. Formulation

A systematic derivation of the QED corrections in a fully relativistic approach requires the use of perturbation theory starting with a one-electron approximation in an effective local potential $V(r)$

$$[-i\boldsymbol{\alpha}\cdot\boldsymbol{\nabla}+\beta m+V(\mathbf{x})]\psi_n(\mathbf{x})=\varepsilon_n\psi_n(\mathbf{x}). \tag{1}$$

In neutral atoms, it is assumed that $V(r)$ includes the interaction with the Coulomb field of the nucleus as well as partly the electron-electron interaction. The interaction of the electrons with the quantized electromagnetic field and the correlation effects are accounted for by the perturbation theory. In this way we obtain quantum electrodynamics in the Furry picture.

To derive formal expressions for the transition amplitude we employ the method developed in Ref. [27] and described in detail in Ref. [28]. While this method is valid for arbitrary many-electron atom and for arbitrary (single, degenerate, and quasidegenerate) initial and final states, its formulation is especially simple for a one-electron atom (or an atom with one electron over the closed shells) and for the case of single initial and final states.

We consider the transition of the atom from the initial state a (which is 6*s* for Cs and 7*s* for Fr) to the final state b (which is 7*s* for Cs and 8*s* for Fr) accompanied by the absorption of a photon with momentum $\mathbf{k}$, energy $k^0=|\mathbf{k}|$, and polarization $\epsilon^\nu=(0,\boldsymbol{\epsilon})$. The transition amplitude is given by the formula [27,28]

$$\tau=Z_3^{-1/2}\frac{1}{2\pi i}\oint_{\Gamma_b}dE'\oint_{\Gamma_a}dE\,g_{b;\gamma,a}(E',E)\times\left[\frac{1}{2\pi i}\oint_{\Gamma_b}dE\,g_{bb}(E)\right]^{-1/2}\left[\frac{1}{2\pi i}\oint_{\Gamma_a}dE\,g_{aa}(E)\right]^{-1/2}. \tag{2}$$

In the case under consideration (one electron over the closed shells), the Green functions $g_{b;\gamma,a}(E',E)$, $g_{aa}(E)$, and $g_{bb}(E)$ are defined by

$$g_{b;\gamma,a}(E',E)\,\delta(E'-E-\omega)=\int d\mathbf{x}\,d\mathbf{x}'\,\psi_a^\dagger(\mathbf{x}')G_\gamma(E',\mathbf{x}';\omega;E,\mathbf{x})\gamma^0\psi_a(\mathbf{x}), \tag{3}$$

$$g_{aa}(E)\,\delta(E'-E)=\frac{2\pi}{i}\int d\mathbf{x}\,d\mathbf{x}'\,\psi_a^\dagger(\mathbf{x}')G(E',\mathbf{x}';E,\mathbf{x})\gamma^0\psi_a(\mathbf{x}), \tag{4}$$

$$g_{bb}(E)\,\delta(E'-E)=\frac{2\pi}{i}\int d\mathbf{x}\,d\mathbf{x}'\,\psi_b^\dagger(\mathbf{x}')G(E',\mathbf{x}';E,\mathbf{x})\gamma^0\psi_b(\mathbf{x}). \tag{5}$$

Here

$$G_\gamma(E',\mathbf{x}';\omega;E,\mathbf{x})=\frac{2\pi}{i}\frac{1}{(2\pi)^3}\int_{-\infty}^{\infty}dx^0dx'^0\int d^4y\times\exp(iE'x'^0-iEx^0-i\omega y^0)\times A^\nu(\mathbf{y})\langle 0|T\psi(x')j_\nu(y)\bar{\psi}(x)|0\rangle \tag{6}$$

is the Fourier transform of the Green function describing the process, $\psi(\mathbf{x})$ is the electron-positron field operator in the Heisenberg representation, $\bar{\psi}=\psi^\dagger\gamma^0$, γ^0 is the Dirac matrix,

$$A^\nu(\mathbf{x})=\frac{\epsilon^\nu\exp(i\mathbf{k}\cdot\mathbf{x})}{\sqrt{2k^0(2\pi)^3}} \tag{7}$$

is the wave function of the absorbed photon, and

$$G(E',\mathbf{x}';E,\mathbf{x})=\frac{1}{(2\pi)^2}\int_{-\infty}^{\infty}dx^0dx'^0\exp(iE'x'^0-iEx^0)\times\langle 0|T\psi(x')\bar{\psi}(x)|0\rangle \tag{8}$$

is the Fourier transform of the Green function describing the atom. The contours Γ_a and Γ_b surround the poles corresponding to the initial and final levels and keep outside all other singularities of the Green functions. It is assumed that they are oriented anticlockwise. Z_3 is the renormalization constant for the photon wave function and the factors $[(1/2\pi i)\oint_{\Gamma_a}dE\,g_{aa}(E)]^{-1/2}$ and $[(1/2\pi i)\oint_{\Gamma_b}dE\,g_{bb}(E)]^{-1/2}$ serve as the normalization factors for the electron wave functions of the states a and b, respectively. The Green functions

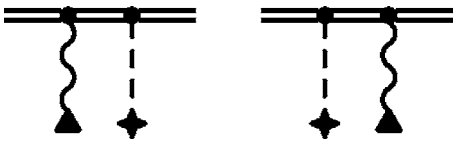

FIG. 1. Feynman diagrams for the lowest-order PNC transition amplitude. The wavy line terminated with a triangle indicates the absorbed photon. The dashed line terminated with a cross indicates the electron-nucleus weak interaction.

G and G_γ are constructed by perturbation theory after the transition to the interaction representation and using Wick's theorem. The Feynman rules for G and G_γ are given in Ref. [28].

To the lowest order, the PNC transition amplitude is described by diagrams presented in Fig 1. Denoting the contribution to $g_{b;\gamma,a}(E',E)$ from these diagrams by $g^{(0)}_{b;\gamma,a}(E',E)$ and taking into account that $g^{(0)}_{aa}=1/(E-\varepsilon_a)$ and $g^{(0)}_{bb}=1/(E-\varepsilon_b)$ and, therefore, the normalization factors in formula (2) are equal to 1, we obtain

$$\tau^{(0)}=\frac{1}{2\pi i}\oint_{\Gamma_b}dE'\oint_{\Gamma_a}dE\,g^{(0)}_{b;\gamma,a}(E',E). \tag{9}$$

According to the Feynman rules [28] and definition (3), we have

$$g^{(0)}_{b;\gamma,a}(E',E)=\frac{i}{2\pi}\frac{1}{E'-\varepsilon_b}\sum_n\frac{\langle b|e\alpha^\nu A_\nu|n\rangle\langle n|H_W|a\rangle}{E-\varepsilon_n}\frac{1}{E-\varepsilon_a}+\frac{i}{2\pi}\frac{1}{E'-\varepsilon_b}\sum_n\frac{\langle b|H_w|n\rangle\langle n|e\alpha^\nu A_\nu|a\rangle}{E'-\varepsilon_n}\frac{1}{E-\varepsilon_a}. \tag{10}$$

Here

$$H_W=-(G_F/\sqrt{8})Q_W\rho_N(r)\gamma_5 \tag{11}$$

is the nuclear spin-independent weak-interaction Hamiltonian [1], G_F is the Fermi constant, γ_5 and $\alpha^\nu\equiv\gamma^0\gamma^\nu=(1,\boldsymbol{\alpha})$ are the Dirac matrices, and ρ_N is the nuclear weak-charge density normalized to unity. Substituting expression (10) into Eq. (9) and taking into account that, for a non-Coulomb potential $V(r)$, there are no states of different parity but of the same energy, we obtain

$$\tau^{(0)}=-\sum_n\left[\frac{\langle b|e\alpha^\nu A_\nu|n\rangle\langle n|H_W|a\rangle}{\varepsilon_a-\varepsilon_n}+\frac{\langle b|H_w|n\rangle\langle n|e\alpha^\nu A_\nu|a\rangle}{\varepsilon_b-\varepsilon_n}\right]. \tag{12}$$

We note here that the case of degenerate levels, that takes place for the pure Coulomb potential, can be considered employing the related formulas from Ref. [28].

The one-loop SE corrections to the PNC transition amplitude are defined by diagrams presented in Fig. 2. To derive the formal expressions for these corrections, one has to expand formula (2) to the next-to-leading order:

$$\tau^{(1)}=\frac{1}{2\pi i}\left\{\oint_{\Gamma_b}dE'\oint_{\Gamma_a}dE\,g^{(1)}_{b;\gamma,a}(E',E)-\frac{1}{2}\oint_{\Gamma_b}dE'\oint_{\Gamma_a}dE\,g^{(0)}_{b;\gamma,a}(E',E)\left[\frac{1}{2\pi i}\oint_{\Gamma_b}dE\,g^{(1)}_{bb}(E)+\frac{1}{2\pi i}\oint_{\Gamma_a}dE\,g^{(1)}_{aa}(E)\right]\right\}. \tag{13}$$

Let us consider the derivation of the contributions from the diagrams "a" and "c." According to the Feynman rules [28], we have

$$g^{(1,a)}_{b;\gamma,a}(E',E)=\frac{i}{2\pi}\frac{1}{E'-\varepsilon_b}\times\sum_{n_1n_2}\frac{\langle b|\Sigma(E')|n_1\rangle\langle n_1|e\alpha^\nu A_\nu|n_2\rangle\langle n_2|H_W|a\rangle}{(E'-\varepsilon_{n_1})(E-\varepsilon_{n_2})}\times\frac{1}{E-\varepsilon_a}, \tag{14}$$

$$g^{(1,c)}_{b;\gamma,a}(E',E)=\frac{i}{2\pi}\frac{1}{E'-\varepsilon_b}\times\sum_{n_1n_2}\frac{\langle b|\Sigma(E')|n_1\rangle\langle n_1|H_W|n_2\rangle\langle n_2|e\alpha^\nu A_\nu|a\rangle}{(E'-\varepsilon_{n_1})(E'-\varepsilon_{n_2})}\times\frac{1}{E-\varepsilon_a}. \tag{15}$$

Here the SE operator is defined as

$$\langle c|\Sigma(E)|d\rangle\equiv\frac{i}{2\pi}\int_{-\infty}^{\infty}d\omega\sum_n\frac{\langle cn|I(\omega)|nd\rangle}{E-\omega-u\varepsilon_n}, \tag{16}$$

where $I(\omega)\equiv e^2\alpha^\mu\alpha^\nu D_{\mu\nu}(\omega)$, $D_{\mu\nu}(\omega)$ is the photon propagator as defined in Ref. [28], and $u=1-i0$ ensures the correct

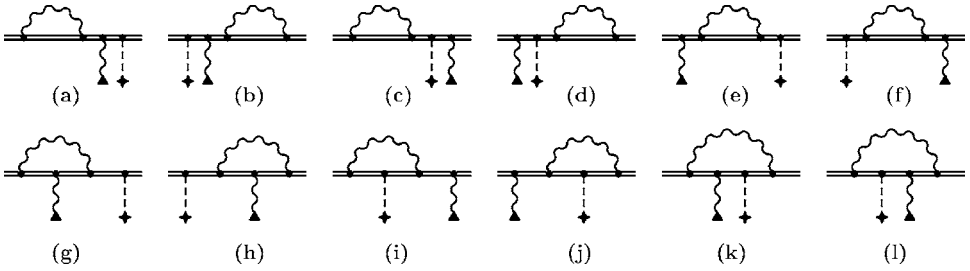

FIG. 2. Feynman diagrams for the SE corrections to the PNC transition amplitude. The wavy line terminated with a triangle indicates the absorbed photon. The dashed line terminated with a cross indicates the electron-nucleus weak interaction.

position of poles of the electron propagators with respect to the integration contour. Taking into account that, for a non-Coulomb potential, the energy ε_{n_2} in Eq. (14) is never equal to ε_a and the energy ε_{n_2} in Eq. (15) is never equal to ε_b, we obtain

$$\oint_{\Gamma_b} dE' \oint_{\Gamma_a} dE\, g^{(1,a)}_{b;\gamma,a}(E',E) = -2\pi i \left[\sum_{n_1,n_2}^{n_1\neq b} \frac{\langle b|\Sigma(\varepsilon_b)|n_1\rangle\langle n_1|e\alpha^\nu A_\nu|n_2\rangle\langle n_2|H_W|a\rangle}{(\varepsilon_b-\varepsilon_{n_1})(\varepsilon_a-\varepsilon_{n_2})} + \sum_n \frac{\langle b|\Sigma'(\varepsilon_b)|b\rangle\langle b|e\alpha^\nu A_\nu|n\rangle\langle n|H_W|a\rangle}{\varepsilon_a-\varepsilon_n} \right], \tag{17}$$

$$\oint_{\Gamma_b} dE' \oint_{\Gamma_a} dE\, g^{(1,c)}_{b;\gamma,a}(E',E) = -2\pi i \left[\sum_{n_1,n_2}^{n_1\neq b} \frac{\langle b|\Sigma(\varepsilon_b)|n_1\rangle\langle n_1|H_W|n_2\rangle\langle n_2|e\alpha^\nu A_\nu|a\rangle}{(\varepsilon_b-\varepsilon_{n_1})(\varepsilon_b-\varepsilon_{n_2})} + \sum_n \frac{\langle b|\Sigma'(\varepsilon_b)|b\rangle\langle b|H_W|n\rangle\langle n|e\alpha^\nu A_\nu|a\rangle}{\varepsilon_b-\varepsilon_n} - \sum_n \frac{\langle b|\Sigma(\varepsilon_b)|b\rangle\langle b|H_W|n\rangle\langle n|e\alpha^\nu A_\nu|a\rangle}{(\varepsilon_b-\varepsilon_n)^2} \right], \tag{18}$$

where $\Sigma'(E)=d\Sigma(E)/dE$. The contributions containing $\langle b|\Sigma'(\varepsilon_b)|b\rangle$ should be considered together with the second term in Eq. (13). Taking into account that

$$\frac{1}{2\pi i}\oint_{\Gamma_b} dE\, g^{(1)}_{bb}(E) = \frac{1}{2\pi i}\oint_{\Gamma_b} dE \frac{\langle b|\Sigma(E)|b\rangle}{(E-\varepsilon_b)^2} = \langle b|\Sigma'(\varepsilon_b)|b\rangle, \tag{19}$$

we obtain

$$-\frac{1}{2}\left[\oint_{\Gamma_b} dE' \oint_{\Gamma_a} dE\, g^{(0)}_{b;\gamma,a}(E',E)\right]\left[\frac{1}{2\pi i}\oint_{\Gamma_b} dE\, \Delta g^{(1)}_{bb}(E)\right] = \frac{1}{2} 2\pi i \sum_n \left[\frac{\langle b|e\alpha^\nu A_\nu|n\rangle\langle n|H_W|a\rangle}{\varepsilon_a-\varepsilon_n} + \frac{\langle b|H_w|n\rangle\langle n|e\alpha^\nu A_\nu|a\rangle}{\varepsilon_b-\varepsilon_n} \right] \langle b|\Sigma'(\varepsilon_b)|b\rangle. \tag{20}$$

Adding this contribution to the terms (17) and (18), we obtain

$$\tau^{(1,a)} = -\left[\sum_{n_1,n_2}^{n_1\neq b} \frac{\langle b|\Sigma(\varepsilon_b)|n_1\rangle\langle n_1|e\alpha^\nu A_\nu|n_2\rangle\langle n_2|H_W|a\rangle}{(\varepsilon_b-\varepsilon_{n_1})(\varepsilon_a-\varepsilon_{n_2})} + \frac{1}{2}\sum_n \frac{\langle b|\Sigma'(\varepsilon_b)|b\rangle\langle b|e\alpha^\nu A_\nu|n\rangle\langle n|H_W|a\rangle}{\varepsilon_a-\varepsilon_n} \right], \tag{21}$$

$$\tau^{(1,c)} = -\left[\sum_{n_1,n_2}^{n_1\neq b} \frac{\langle b|\Sigma(\varepsilon_b)|n_1\rangle\langle n_1|H_W|n_2\rangle\langle n_2|e\alpha^\nu A_\nu|a\rangle}{(\varepsilon_b-\varepsilon_{n_1})(\varepsilon_b-\varepsilon_{n_2})} + \frac{1}{2}\sum_n \frac{\langle b|\Sigma'(\varepsilon_b)|b\rangle\langle b|H_W|n\rangle\langle n|e\alpha^\nu A_\nu|a\rangle}{\varepsilon_b-\varepsilon_n} - \sum_n \frac{\langle b|\Sigma(\varepsilon_b)|b\rangle\langle b|H_W|n\rangle\langle n|e\alpha^\nu A_\nu|a\rangle}{(\varepsilon_b-\varepsilon_n)^2} \right]. \tag{22}$$

Similar calculations yield

$$\tau^{(1,b)} = -\left[\sum_{n_1,n_2}^{n_2\neq a} \frac{\langle b|H_W|n_1\rangle\langle n_1|e\alpha^\nu A_\nu|n_2\rangle\langle n_2|\Sigma(\varepsilon_a)|a\rangle}{(\varepsilon_b-\varepsilon_{n_1})(\varepsilon_a-\varepsilon_{n_2})} + \frac{1}{2}\sum_n \frac{\langle b|H_W|n\rangle\langle n|e\alpha^\nu A_\nu|a\rangle\langle a|\Sigma'(\varepsilon_a)|a\rangle}{\varepsilon_b-\varepsilon_n} \right], \tag{23}$$

$$\tau^{(1,d)} = -\left[\sum_{n_1,n_2}^{n_1\neq b} \frac{\langle b|e\alpha^\nu A_\nu|n_1\rangle\langle n_1|H_W|n_2\rangle\langle n_2|\Sigma(\varepsilon_a)|a\rangle}{(\varepsilon_a-\varepsilon_{n_1})(\varepsilon_a-\varepsilon_{n_2})} + \frac{1}{2}\sum_n \frac{\langle b|e\alpha^\nu A_\nu|n\rangle\langle n|H_W|a\rangle\langle a|\Sigma'(\varepsilon_a)|a\rangle}{\varepsilon_a-\varepsilon_n} - \sum_n \frac{\langle b|e\alpha^\nu A_\nu|n\rangle\langle n|H_W|a\rangle\langle a|\Sigma(\varepsilon_a)|a\rangle}{(\varepsilon_a-\varepsilon_n)^2} \right], \tag{24}$$

$$\tau^{(1,e)} = -\sum_{n_1,n_2}^{n_1\neq b} \frac{\langle b|e\alpha^\nu A_\nu|n_1\rangle\langle n_1|\Sigma(\varepsilon_a)|n_2\rangle\langle n_2|H_W|a\rangle}{(\varepsilon_a-\varepsilon_{n_1})(\varepsilon_a-\varepsilon_{n_2})}, \tag{25}$$

$$\tau^{(1,f)} = -\sum_{n_1,n_2}^{n_2\neq a} \frac{\langle b|H_W|n_1\rangle\langle n_1|\Sigma(\varepsilon_b)|n_2\rangle\langle n_2|e\alpha^\nu A_\nu|a\rangle}{(\varepsilon_b-\varepsilon_{n_1})(\varepsilon_b-\varepsilon_{n_2})}, \tag{26}$$

$$\tau^{(1,g)} = -\frac{i}{2\pi}\int_{-\infty}^{\infty} d\omega \sum_{n,n_1,n_2} \frac{\langle n_1|e\alpha^\nu A_\nu|n_2\rangle\langle n|H_W|a\rangle}{(\varepsilon_a-\varepsilon_n)} \times \frac{\langle bn_2|I(\omega)|n_1n\rangle}{[\varepsilon_b-\omega-u\varepsilon_{n_1}][\varepsilon_a-\omega-u\varepsilon_{n_2}]}, \tag{27}$$

$$\tau^{(1,h)} = -\frac{i}{2\pi}\int_{-\infty}^{\infty} d\omega \sum_{n,n_1,n_2} \frac{\langle b|H_W|n\rangle\langle n_1|e\alpha^\nu A_\nu|n_2\rangle}{(\varepsilon_b-\varepsilon_n)} \times \frac{\langle nn_2|I(\omega)|n_1a\rangle}{[\varepsilon_b-\omega-u\varepsilon_{n_1}][\varepsilon_a-\omega-u\varepsilon_{n_2}]}, \tag{28}$$

$$\tau^{(1,i)} = -\frac{i}{2\pi}\int_{-\infty}^{\infty} d\omega \sum_{n,n_1,n_2} \frac{\langle n_1|H_W|n_2\rangle\langle n|e\alpha^\nu A_\nu|a\rangle}{(\varepsilon_b-\varepsilon_n)} \times \frac{\langle bn_2|I(\omega)|n_1n\rangle}{[\varepsilon_b-\omega-u\varepsilon_{n_1}][\varepsilon_b-\omega-u\varepsilon_{n_2}]}, \tag{29}$$

$$\tau^{(1,j)} = -\frac{i}{2\pi}\int_{-\infty}^{\infty} d\omega \sum_{n,n_1,n_2} \frac{\langle b|e\alpha^\nu A_\nu|n\rangle\langle n_1|H_W|n_2\rangle}{(\varepsilon_a-\varepsilon_n)} \times \frac{\langle nn_2|I(\omega)|n_1a\rangle}{[\varepsilon_a-\omega-u\varepsilon_{n_1}][\varepsilon_a-\omega-u\varepsilon_{n_2}]}, \tag{30}$$

$$\tau^{(1,k)} = -\frac{i}{2\pi}\int_{-\infty}^{\infty} d\omega \sum_{n_1,n_2,n_3} \frac{\langle bn_2|I(\omega)|n_1a\rangle}{[\varepsilon_b-\omega-u\varepsilon_{n_1}]} \times \frac{\langle n_1|e\alpha^\nu A_\nu|n_3\rangle\langle n_3|H_W|n_2\rangle}{[\varepsilon_a-\omega-u\varepsilon_{n_3}][\varepsilon_a-\omega-u\varepsilon_{n_2}]}, \tag{31}$$

$$\tau^{(1,l)} = -\frac{i}{2\pi}\int_{-\infty}^{\infty} d\omega \sum_{n_1,n_2,n_3} \frac{\langle bn_2|I(\omega)|n_1a\rangle}{[\varepsilon_b-\omega-u\varepsilon_{n_1}]} \times \frac{\langle n_1|H_W|n_3\rangle\langle n_3|e\alpha^\nu A_\nu|n_2\rangle}{[\varepsilon_b-\omega-u\varepsilon_{n_3}][\varepsilon_a-\omega-u\varepsilon_{n_2}]}. \tag{32}$$

Taking into account the corresponding diagrams with the mass counterterm results in the replacement $\Sigma(E)\to\Sigma_{\rm R}(E)=\Sigma(E)-\gamma^0\delta m$.

Since the wave length of the absorbed photon is much larger than the atomic size, one can use the dipole approximation. It means the replacement $\exp(i\mathbf{k}\cdot\mathbf{x})\to 1$ in the photon wave function and, therefore, $e\alpha^\nu A_\nu\to|e|(\boldsymbol{\alpha}\cdot\boldsymbol{\epsilon})/\sqrt{2k^0(2\pi)^3}$ in formulas (12) and (21)–(32). Within this approximation, the corresponding formulas in the length gauge are obtained by replacing $\boldsymbol{\alpha}$ with $\mathbf{r}$ in all vertices corresponding to the photon absorption and by multiplying the amplitude (12) with the factor $i(E_b-E_a)$, where $E_a=\varepsilon_a+\langle a|\Sigma_{\rm R}(\varepsilon_a)|a\rangle$ and $E_b=\varepsilon_b+\langle b|\Sigma_{\rm R}(\varepsilon_b)|b\rangle$, and the amplitudes (21)–(32) with the factor $i(\varepsilon_b-\varepsilon_a)$. This prescription can be derived from Eqs. (12) and (21)–(32) employing the commutation relation $\boldsymbol{\alpha}=i[h_{\rm D},\mathbf{r}]$, where $h_{\rm D}=-i\boldsymbol{\alpha}\cdot\boldsymbol{\nabla}+\beta m+V(r)$ is the Dirac Hamiltonian. Alternatively, one can get the prescription, using Eq. (205) of Ref. [28] and the equal-time commutation relations for the field operators in the Heisenberg representation.

The theoretical and experimental results for the PNC amplitude in alkali-metal atoms are generally presented in terms of the $E_{\rm PNC}$ amplitude which is defined as the matrix element of the z component of the atomic electric-dipole moment between the initial (a) and final (b) s states with the angular momentum projections $m_a=m_b=\frac{1}{2}$. It is related to the τ amplitude by the equation

$$E_{\rm PNC} = i\tau[e\alpha^\nu A_\nu\to e\alpha_z]/(E_b-E_a) = \tau[e\alpha^\nu A_\nu\to -d_z], \tag{33}$$

where the s states a and b have the angular momentum projections $m_a=m_b=\frac{1}{2}$, E_a and E_b are their total energies, and $d_z=ez$ is the z component of the dipole moment operator ($e<0$). To the zeroth order, one easily finds

$$E_{\rm PNC} = \sum_n \left[\frac{\langle b|d_z|n\rangle\langle n|H_W|a\rangle}{\varepsilon_a-\varepsilon_n} + \frac{\langle b|H_W|n\rangle\langle n|d_z|a\rangle}{\varepsilon_b-\varepsilon_n}\right]. \tag{34}$$

The one-loop SE correction is given by the sum of the following terms:

$$\delta E^{\rm a}_{\rm PNC} = \sum_{n_1,n_2}^{(n_1\neq b)} \frac{\langle b|\Sigma_{\rm R}(\varepsilon_b)|n_1\rangle\langle n_1|d_z|n_2\rangle\langle n_2|H_W|a\rangle}{(\varepsilon_b-\varepsilon_{n_1})(\varepsilon_a-\varepsilon_{n_2})} + \frac{1}{2}\sum_n \frac{\langle b|\Sigma'_{\rm R}(\varepsilon_b)|b\rangle\langle b|d_z|n\rangle\langle n|H_W|a\rangle}{(\varepsilon_a-\varepsilon_n)}, \tag{35}$$

$$\delta E^{\rm b}_{\rm PNC} = \sum_{n_1,n_2}^{(n_2\neq a)} \frac{\langle b|H_W|n_1\rangle\langle n_1|d_z|n_2\rangle\langle n_2|\Sigma_{\rm R}(\varepsilon_a)|a\rangle}{(\varepsilon_b-\varepsilon_{n_1})(\varepsilon_a-\varepsilon_{n_2})} + \frac{1}{2}\sum_n \frac{\langle b|H_W|n\rangle\langle n|d_z|a\rangle\langle a|\Sigma'_{\rm R}(\varepsilon_a)|a\rangle}{(\varepsilon_b-\varepsilon_n)}, \tag{36}$$

$$\delta E^{\rm c}_{\rm PNC} = \sum_{n_1,n_2}^{(n_1\neq b)} \frac{\langle b|\Sigma_{\rm R}(\varepsilon_b)|n_1\rangle\langle n_1|H_W|n_2\rangle\langle n_2|d_z|a\rangle}{(\varepsilon_b-\varepsilon_{n_1})(\varepsilon_b-\varepsilon_{n_2})} + \frac{1}{2}\sum_n \frac{\langle b|\Sigma'_{\rm R}(\varepsilon_b)|b\rangle\langle b|H_W|n\rangle\langle n|d_z|a\rangle}{(\varepsilon_b-\varepsilon_n)} - \sum_n \frac{\langle b|\Sigma_{\rm R}(\varepsilon_b)|b\rangle\langle b|H_W|n\rangle\langle n|d_z|a\rangle}{(\varepsilon_b-\varepsilon_n)^2}, \tag{37}$$

$$\delta E^{\rm d}_{\rm PNC} = \sum_{n_1,n_2}^{(n_2\neq a)} \frac{\langle b|d_z|n_1\rangle\langle n_1|H_W|n_2\rangle\langle n_2|\Sigma_{\rm R}(\varepsilon_a)|a\rangle}{(\varepsilon_a-\varepsilon_{n_1})(\varepsilon_a-\varepsilon_{n_2})} + \frac{1}{2}\sum_n \frac{\langle b|d_z|n\rangle\langle n|H_W|a\rangle\langle a|\Sigma'_{\rm R}(\varepsilon_a)|a\rangle}{(\varepsilon_a-\varepsilon_n)} - \sum_n \frac{\langle b|d_z|n\rangle\langle n|H_W|a\rangle\langle a|\Sigma_{\rm R}(\varepsilon_a)|a\rangle}{(\varepsilon_a-\varepsilon_n)^2}, \tag{38}$$

$$\delta E^{\rm e}_{\rm PNC} = \sum_{n_1,n_2} \frac{\langle b|d_z|n_1\rangle\langle n_1|\Sigma_{\rm R}(\varepsilon_a)|n_2\rangle\langle n_2|H_W|a\rangle}{(\varepsilon_a-\varepsilon_{n_1})(\varepsilon_a-\varepsilon_{n_2})}, \tag{39}$$

$$\delta E^{\rm f}_{\rm PNC} = \sum_{n_1,n_2} \frac{\langle b|H_W|n_1\rangle\langle n_1|\Sigma_{\rm R}(\varepsilon_b)|n_2\rangle\langle n_2|d_z|a\rangle}{(\varepsilon_b-\varepsilon_{n_1})(\varepsilon_b-\varepsilon_{n_2})}, \tag{40}$$

$$\delta E^{\rm g}_{\rm PNC} = \frac{i}{2\pi}\int_{-\infty}^{\infty} d\omega \sum_{n,n_1,n_2} \frac{\langle n_1|d_z|n_2\rangle\langle n|H_W|a\rangle}{(\varepsilon_a-\varepsilon_n)} \times \frac{\langle bn_2|I(\omega)|n_1n\rangle}{[\varepsilon_b-\omega-u\varepsilon_{n_1}][\varepsilon_a-\omega-u\varepsilon_{n_2}]}, \tag{41}$$

$$\delta E^{\rm h}_{\rm PNC} = \frac{i}{2\pi}\int_{-\infty}^{\infty} d\omega \sum_{n,n_1,n_2} \frac{\langle b|H_W|n\rangle\langle n_1|d_z|n_2\rangle}{(\varepsilon_b-\varepsilon_n)} \times \frac{\langle nn_2|I(\omega)|n_1a\rangle}{[\varepsilon_b-\omega-u\varepsilon_{n_1}][\varepsilon_a-\omega-u\varepsilon_{n_2}]}, \tag{42}$$

$$\delta E^{\mathrm{i}}_{\mathrm{PNC}} = \frac{i}{2\pi}\int_{-\infty}^{\infty} d\omega \sum_{n,n_1,n_2} \frac{\langle n_1|H_W|n_2\rangle\langle n|d_z|a\rangle}{(\varepsilon_b-\varepsilon_n)} \times \frac{\langle bn_2|I(\omega)|n_1 n\rangle}{[\varepsilon_b-\omega-u\varepsilon_{n_1}][\varepsilon_b-\omega-u\varepsilon_{n_2}]}, \tag{43}$$

$$\delta E^{\mathrm{j}}_{\mathrm{PNC}} = \frac{i}{2\pi}\int_{-\infty}^{\infty} d\omega \sum_{n,n_1,n_2} \frac{\langle b|d_z|n\rangle\langle n_1|H_W|n_2\rangle}{(\varepsilon_a-\varepsilon_n)} \times \frac{\langle nn_2|I(\omega)|n_1 a\rangle}{[\varepsilon_a-\omega-u\varepsilon_{n_1}][\varepsilon_a-\omega-u\varepsilon_{n_2}]}, \tag{44}$$

$$\delta E^{\mathrm{k}}_{\mathrm{PNC}} = \frac{i}{2\pi}\int_{-\infty}^{\infty} d\omega \sum_{n_1,n_2,n_3} \frac{\langle bn_2|I(\omega)|n_1 a\rangle}{[\varepsilon_b-\omega-u\varepsilon_{n_1}]} \times \frac{\langle n_1|d_z|n_3\rangle\langle n_3|H_W|n_2\rangle}{[\varepsilon_a-\omega-u\varepsilon_{n_3}][\varepsilon_a-\omega-u\varepsilon_{n_2}]}, \tag{45}$$

$$\delta E^{\mathrm{l}}_{\mathrm{PNC}} = \frac{i}{2\pi}\int_{-\infty}^{\infty} d\omega \sum_{n_1,n_2,n_3} \frac{\langle bn_2|I(\omega)|n_1 a\rangle}{[\varepsilon_b-\omega-u\varepsilon_{n_1}]} \times \frac{\langle n_1|H_W|n_3\rangle\langle n_3|d_z|n_2\rangle}{[\varepsilon_b-\omega-u\varepsilon_{n_3}][\varepsilon_a-\omega-u\varepsilon_{n_2}]}. \tag{46}$$

According to Eq. (33), the corresponding expressions in the velocity gauge are obtained by the replacement $d_z \to -ie\alpha_z/(E_b-E_a)$, where the energies E_a and E_b include the SE corrections. In addition to the replacement $d_z \to -ie\alpha_z/(\varepsilon_b-\varepsilon_a)$ in Eqs. (34)–(46), it yields the contribution

$$\delta E^{\mathrm{add}}_{\mathrm{PNC}} = -\frac{\langle b|\Sigma_{\mathrm{R}}(\varepsilon_b)|b\rangle - \langle a|\Sigma_{\mathrm{R}}(\varepsilon_a)|a\rangle}{\varepsilon_b-\varepsilon_a} E_{\mathrm{PNC}}, \tag{47}$$

which results from the expansion

$$\frac{1}{E_b-E_a} \approx \frac{1}{\varepsilon_b-\varepsilon_a}\left[1-\frac{\langle b|\Sigma_{\mathrm{R}}(\varepsilon_b)|b\rangle - \langle a|\Sigma_{\mathrm{R}}(\varepsilon_a)|a\rangle}{(\varepsilon_b-\varepsilon_a)}\right]. \tag{48}$$

It can be shown that the sum of contributions (43)–(46) is the same in the length and the velocity gauge. Because of the gauge invariance of the total SE correction, the same is valid for the sum of the other terms, Eqs. (35)–(42) and (47).

Formulas (35)–(47) contain ultraviolet and infrared divergences. To cancel the ultraviolet divergences, we expand contributions (35)–(40) into zero-, one-, and many-potential terms and contributions (41)–(44) into zero- and many-potential terms. The ultraviolet divergencies are present only in the zero- and one-potential terms. They are removed analytically by calculating these terms in the momentum space (for details, we refer to Refs. [29–31]). For the standard zero- and one-potential terms we employ the equations given in Ref. [30], whereas the corresponding expression for the zero-potential PNC term is presented in the Appendix. The many-potential terms are evaluated in configuration space employing the Wick rotation in the complex ω plane. The infrared divergences, which occur in contributions (35)–(38), (45), and (46), are regularized by introducing a nonzero photon mass and cancelled analytically.

The expressions for the VP corrections, which do not contain any insertions with the external photon line or the weak interaction attached to the electron loop, are obtained from Eqs. (35)–(40) by the replacement of the SE operator with the VP potential. The other VP corrections will not be considered here, since their contribution is negligible. To a high accuracy, the VP potential is determined by the Uehling term, which corresponds to the first nonzero term in the expansion of the vacuum loop in powers of the Coulomb potential. The renormalized expression for the Uehling potential is

$$U_{\mathrm{Uehl}}(r) = -\alpha Z\frac{2\alpha}{3\pi}\int_0^{\infty} dr' 4\pi r'\rho(r')\int_1^{\infty} dt\left(1+\frac{1}{2t^2}\right)\frac{\sqrt{t^2-1}}{t^2} \times \frac{\{\exp(-2m|r-r'|t)-\exp[-2m(r+r')t]\}}{4mrt}, \tag{49}$$

where $\rho(r)$ is the nuclear charge density, normalized to unity. To account for the screening effect on the Uehling potential, one should replace $Z\rho(r)$ by $Z\rho(r)-(Z-1)\rho_{\mathrm{core}}(r)$, where $\rho_{\mathrm{core}}(r)$ is the charge density of the core electrons, normalized to unity. The higher-order one-loop VP potential, the so-called Wichmann-Kroll term, can be evaluated for the point-charge nucleus using approximate formulas derived in Ref. [32].

B. Local Dirac-Fock potential

Since the energy intervals between the levels $6s$, $6p_{1/2}$, $7s$, and $7p_{1/2}$ in Cs and the levels $7s$, $7p_{1/2}$, $8s$, and $8p_{1/2}$ in Fr are very small, to get reliable results for the transition amplitudes under consideration, one needs to use a local potential $V(r)$ that reproduces energies and wave functions of these states on the Dirac-Fock accuracy level or better. We construct such a potential by inverting the radial Dirac equation with the radial wave function obtained by solving the DF equation with the code of Ref. [33].

The radial DF equations have the form [33]

$$-\left(\frac{d}{dr}-\frac{\kappa_a}{r}\right)F_a+\left(V_{\mathrm{C}}+\frac{Y_a(r)}{r}\right)G_a+mG_a=\varepsilon_a G_a-\frac{X^F_a}{r},$$

$$\left(\frac{d}{dr}+\frac{\kappa_a}{r}\right)G_a+\left(V_{\mathrm{C}}+\frac{Y_a(r)}{r}\right)F_a-mF_a=\varepsilon_a F_a-\frac{X^G_a}{r}. \tag{50}$$

Here $G_a/r=g_a$ and $F_a/r=f_a$ are the large and small radial components of the Dirac wave function of the a shell electron, ε_a is the one-electron energy, $\kappa_a=(-1)^{j+l+1/2}(j+\frac{1}{2})$ is the relativistic quantum number, V_{C} is the Coulomb potential induced by the nucleus, and $Y_a(r)/r$ is the screening potential. The functions X^G_a and X^F_a consist of two parts. The first part is the result of the action of the exchange-interaction operator on the radial wave functions G_a and F_a. The second part is the contribution from the nondiagonal Lagrangian

multipliers, which provide the orthogonality of the radial wave functions corresponding to different values of the principal quantum number n_a but the same κ_a. The functions X_a^G and X_a^F are calculated self-consistently from the DF equations employng the radial wave functions obtained at the previous iteration step.

Let us consider the Dirac equation for the a shell electron with a local potential $V_a(r)$:

$$-\left(\frac{d}{dr}-\frac{\kappa_a}{r}\right)F_a+V_a(r)G_a+mG_a=\varepsilon_a G_a,$$

$$\left(\frac{d}{dr}+\frac{\kappa_a}{r}\right)G_a+V_a(r)F_a-mF_a=\varepsilon_a F_a. \tag{51}$$

In contrast to the nonrelativistic Schrödinger equation, generally speaking, it is impossible to choose such a local potential $V_a(r)$ which would exactly reproduce the one-electron energy ε_a and the radial components G_a and F_a for a given shell. This is due to the fact that the potential $V_a(r)$ enters both radial equations. However, one can derive an approximate potential by inverting the radial Dirac equation for the large component:

$$V_a^0(r)=\varepsilon_a-m+\frac{1}{G_a}\left(\frac{d}{dr}-\frac{\kappa_a}{r}\right)F_a=V_{\mathrm{C}}+\frac{Y_a(r)}{r}+\frac{1}{G_a r}X_a^F. \tag{52}$$

This leads to a local potential $V_a^0(r)$ which has some singularities, because the function G_a has nodes in the core region for $n_a>l_a+1$.

Let us consider another method of constructing the potential $V_a(r)$. Multiplying the first and second radial Dirac equations with G_a and F_a, respectively, and summing them, we obtain

$$-G_a\left(\frac{d}{dr}-\frac{\kappa_a}{r}\right)F_a+F_a\left(\frac{d}{dr}+\frac{\kappa_a}{r}\right)G_a+V_a(r)\rho_a+mG_a^2-mF_a^2=\varepsilon_a\rho_a, \tag{53}$$

where $\rho_a=G_a^2+F_a^2$. Inverting this equation with respect to $V_a(r)$, we have

$$V_a^{(1)}(r)=\varepsilon_a+\frac{G_a}{\rho_a}\left(\frac{d}{dr}-\frac{\kappa_a}{r}\right)F_a-\frac{F_a}{\rho_a}\left(\frac{d}{dr}+\frac{\kappa_a}{r}\right)G_a+m\frac{F_a^2}{\rho_a}-m\frac{G_a^2}{\rho_a}=V_{\mathrm{C}}+\frac{Y_a(r)}{r}+\frac{1}{\rho_a r}(G_aX_a^F+F_aX_a^G). \tag{54}$$

Despite that the potential $V_a^{(1)}(r)$ has no singularities in the core region, it can oscillate and singularities can occur in the nonrelativistic limit.

To smooth the potential $V_a^{(1)}(r)$ in the core region, we use the following procedure. Instead of the density ρ_a, we consider an average density $\bar{\rho}_a$ defined by

TABLE I. The binding energies of low-lying states in Cs, in a.u. The experimental energies are taken from Ref. [34]

State	Local potential	DF	Expt.
$6s_{1/2}$	−0.13079	−0.12824	−0.14310
$6p_{1/2}$	−0.08696	−0.08582	−0.09217
$6p_{3/2}$	−0.08479	−0.08397	−0.08965
$7s_{1/2}$	−0.05621	−0.05537	−0.05865
$7p_{1/2}$	−0.04251	−0.04209	−0.04393
$7p_{3/2}$	−0.04175	−0.04143	−0.04310

$$\bar{\rho}_{n_a\kappa_a}=\sum_{n\leqslant n_a} w_{n\kappa_a}\rho_{n\kappa_a},\quad \sum_{n\leqslant n_a} w_{n\kappa_a}=1, \tag{55}$$

where $w_{n\kappa_a}$ are positive weights. Thus, the density $\rho_{n_a\kappa_a}$ gets some admixture of the densities of the core shells corresponding to the same value of κ_a but different values of the principal quantum number $n<n_a$. Since the maximal values of the core shell densities are located nearby the nodes of the function G_a, the density $\bar{\rho}_{n_a\kappa_a}$ can be made to be smooth and nodeless by a proper choice of the weights $w_{n\kappa_a}$. Outside the core region the densities $\rho_{n_a\kappa_a}$ and $\bar{\rho}_{n_a\kappa_a}$ almost coincide with each other. This is due to a fast decrease of the core wave functions outside the core. Assuming the nonlocal part of the DF potential can be replaced by a local potential which is the same for all shells with the same κ_a, one can derive

$$V_a^{(2)}(r)=V_{\mathrm{C}}+\frac{Y_a(r)}{r}+\frac{1}{\bar{\rho}_{n_a\kappa_a}r}\sum_{n\leqslant n_a} w_{n\kappa_a}(G_{n\kappa_a}X^F_{n\kappa_a}+F_{n_a\kappa_a}X^G_{n\kappa_a}). \tag{56}$$

The potential $V_a^{(2)}(r)$ derived for the shell a can also be used for all shells with the same and different values of κ_a. This potential with weights $w_{n\kappa_a}\propto(m-\varepsilon_{n_a\kappa_a})/(m-\varepsilon_{n\kappa_a})$ was used in our calculations.

In Table I, we compare the energies of the cesium atom obtained with the local potential $V(r)$, that was derived using mainly the DF wave function of the $6s$ state, with the DF energies and with the experimental ones. The corresponding comparision for the francium atom, where the local potential was derived using mainly the DF wave function of the $7s$ state, is presented in Table II.

TABLE II. The binding energies of low-lying states in Fr, in a.u.

State	Local potential	DF	Expt. [35–41]
$7s_{1/2}$	−0.13640	−0.13271	−0.14967
$7p_{1/2}$	−0.08857	−0.08629	−0.09391
$7p_{3/2}$	−0.08199	−0.08071	−0.08623
$8s_{1/2}$	−0.05740	−0.05626	−0.05976
$8p_{1/2}$	−0.04297	−0.04222	−0.04436
$8p_{3/2}$	−0.04071	−0.04023	−0.04188

TABLE III. The SE corrections to the 6*s*-7*s* PNC amplitude in Cs and to the 7*s*-8*s* PNC amplitude in Fr, in %. The results are presented in both the length (*L*) and the velocity (*V*) gauge.

	Cs		Fr	
Contribution	*L* gauge	*V* gauge	*L* gauge	*V* gauge
δE^{a}_{PNC}	−0.09	−0.11	0.18	0.15
δE^{b}_{PNC}	1.31	1.11	1.84	1.35
δE^{c}_{PNC}	0.34	0.40	−0.36	−0.23
δE^{d}_{PNC}	−0.38	−0.32	−0.64	−0.51
δE^{e}_{PNC}	−1.29	−1.53	−1.21	−1.46
δE^{f}_{PNC}	3.89	3.25	3.61	2.94
δE^{g}_{PNC}	1.33	1.57	1.32	1.58
δE^{h}_{PNC}	−4.04	−3.40	−4.03	−3.36
δE^{i}_{PNC}	−4.61	−3.97	−4.97	−4.30
δE^{j}_{PNC}	1.49	1.73	1.58	1.83
δE^{k}_{PNC}	−0.79	−1.03	−0.78	−1.04
δE^{l}_{PNC}	2.05	1.41	2.05	1.38
δE^{add}_{PNC}	0.00	0.10	0.00	0.26
δE^{tot}_{PNC}	−0.79	−0.79	−1.40	−1.40

C. Numerical evaluation of the QED corrections

Numerical evaluation of expressions (34)–(47) was performed by employing the dual-kinetic-balance finite basis set method [42] with basis functions construced from *B* splines. The calculation of the zeroth-order contribution (34), with $V(r)$ constructed as indicated above, yields $E_{PNC}=-1.002$ for ^{133}Cs and $E_{PNC}=-10.19$ for ^{223}Fr, in units of $i\times10^{-11}(-Q_W)/N$ a.u. These values should be compared with the corresponding DF values, −0.741 for ^{133}Cs and −13.72 for ^{223}Fr, and with the values that include the correlation effects, −0.904 for ^{133}Cs and −15.72 for ^{223}Fr (see the next section). The individual SE corrections are presented in Table III. Since there is a significant cancellation between terms containing the infrared singularities, the terms corresponding to $n=a$ in $\Sigma'_R(\varepsilon_a)$ and $n=b$ in $\Sigma'_R(\varepsilon_b)$ are subtracted from contributions (35)–(38) and added to contributions (45) and (46). The total SE correction δE^{tot}_{PNC}, presented in Table III, contains also the free term, $-\alpha/(2\pi)E_{PNC}$, mentioned above. Since this term is usually included into the weak charge Q_W, one has to consider the binding SE correction defined as $\delta E^{bind}_{PNC}=\delta E^{tot}_{PNC}+\alpha/(2\pi)E_{PNC}$. According to our calculations, the binding SE correction amounts to −0.67% for cesium and −1.29% for francium. To estimate the uncertainty of these values due to correlation effects, we have also performed the calculations with $V(r)$ constructed employing the DF wave function of the 7*s* state for cesium and the 8*s* state for francium. While this leads to a 2% decrease of the transition amplitude, the relative shift of the SE correction is, however, five times smaller. Since the correlation effects contribute to the transition amplitude on the 20% level, we assume a 4% uncertainty for the total SE correction. Therefore, our value for the binding SE correction is −0.67(3)% for cesium and −1.29(5)% for francium. In the case of cesium, our value differs from the previous evaluations of the SE effect, which are −0.9(1)% [20] and −0.85% [19].

TABLE IV. The Uehling corrections to the 6*s*-7*s* PNC amplitude in Cs and to the 7*s*-8*s* PNC amplitude in Fr, in %. The results are presented in both the length (*L*) and the velocity (*V*) gauge.

	Cs		Fr	
Contribution	*L* gauge	*V* gauge	*L* gauge	*V* gauge
δE^{a}_{PNC}	−0.026	−0.024	−0.107	−0.100
δE^{b}_{PNC}	−0.050	−0.024	−0.208	−0.098
δE^{c}_{PNC}	0.354	0.347	0.930	0.902
δE^{d}_{PNC}	−0.054	−0.061	−0.077	−0.107
δE^{e}_{PNC}	−0.070	−0.069	−0.188	−0.188
δE^{f}_{PNC}	0.255	0.256	0.687	0.687
δE^{add}_{PNC}	0	−0.014	0	−0.060
δE^{tot}_{PNC}	0.410	0.410	1.037	1.037

We have also calculated the VP correction. The individual contributions for the Uehling part, calculated including the screening correction as described after Eq. (49), are presented in Table IV. The total Uehling correction is almost independent of the screening effect and amounts to 0.410% for cesium and 1.037% for francium. These results agree well with the previous calculations of this correction. The individual contributions for the Wichmann-Kroll (WK) correction, obtained employing approximate formulas for the WK potential from Ref. [32], are given in Table V. The total WK correction is equal to −0.004% (cf. [13]) for cesium and −0.028% for francium. This leads to the 0.406% result for the total VP correction for cesium and to the 1.01% result for francium. Therefore, the total binding QED correction amounts to −0.27(3)% for cesium and −0.28(5)% for francium.

III. ELECTRON CORRELATION EFFECT ON THE PNC TRANSITION AMPLITUDE

To calculate the correlation effects on the PNC amplitude we start with the relativistic Hamiltonian in the no-pair approximation:

TABLE V. The Wichmann-Kroll corrections to the 6*s*-7*s* PNC amplitude in Cs and to the 7*s*-8*s* PNC amplitude in Fr, in %. The results are presented in both the length (*L*) and the velocity (*V*) gauge.

	Cs		Fr	
Contribution	*L* gauge	*V* gauge	*L* gauge	*V* gauge
δE^{a}_{PNC}	0.0006	0.0006	0.0053	0.0049
δE^{b}_{PNC}	0.0012	0.0006	0.0102	0.0048
δE^{c}_{PNC}	−0.0042	−0.0041	−0.0284	−0.0270
δE^{d}_{PNC}	0.0001	0.0003	−0.0009	0.0006
δE^{e}_{PNC}	0.0007	0.0007	0.0055	0.0055
δE^{f}_{PNC}	−0.0026	−0.0026	−0.0199	−0.0199
δE^{add}_{PNC}	0	0.0003	0	0.0030
δE^{tot}_{PNC}	−0.0042	−0.0042	−0.0283	−0.0283

$$H_{\rm np} = \Lambda_+ H \Lambda_+, \quad H = \sum_j h_{\rm D}(j) + V_{\rm C}^{\rm int} + V_{\rm B}^{\rm int}, \tag{57}$$

where $h_{\rm D}$ is the one-electron Dirac Hamiltonian, the index $j=1,\ldots,N$ enumerates the electrons, and $V_{\rm C}^{\rm int}$ and $V_{\rm B}^{\rm int}$ are the Coulomb and the Breit electron-electron interaction operator, respectively. The frequency-independent Breit interaction in the Coulomb gauge is given by

$$V_{\rm B}^{\rm int} = V_{\rm G}^{\rm int} + V_{\rm R}^{\rm int}, \quad V_{\rm G}^{\rm int} = -\alpha \sum_{i<j} \frac{\boldsymbol{\alpha}_i \cdot \boldsymbol{\alpha}_j}{r_{ij}},$$

$$V_{\rm R}^{\rm int} = -\frac{\alpha}{2} \sum_{i<j} (\boldsymbol{\alpha}_i \cdot \boldsymbol{\nabla}_i)(\boldsymbol{\alpha}_j \cdot \boldsymbol{\nabla}_j) r_{ij}. \tag{58}$$

Here $V_{\rm G}^{\rm int}$ is the so-called magnetic or Gaunt term and $V_{\rm R}^{\rm int}$ is the retardation term. The operator Λ_+ is the projector on the positive-energy states, which is the product of the one-electron projectors $\lambda_+(i)$,

$$\Lambda_+ = \lambda_+(1) \cdots \lambda_+(N), \tag{59}$$

where

$$\lambda_+(i) = \sum_n |u_n(i)\rangle\langle u_n(i)|. \tag{60}$$

Here $u_n(i)$ are the positive-energy eigenstates of an effective one-particle Hamiltonian h_u,

$$h_u u_n = \varepsilon_n u_n, \tag{61}$$

which can be taken to be the Dirac Hamiltonian $h_{\rm D}$, the Dirac Hamiltonian in an external field, or the DF Hamiltonian in an external field [43–45].

To calculate the $E_{\rm PNC}$ amplitude, we add the weak interaction to the full Hamiltonian:

$$H(\mu) = H + \mu \sum_j H_W(j), \tag{62}$$

where H_W is defined by Eq. (11).

With the PNC interaction added to the one-electron DF Hamiltonian, one obtains the coupled equations, which are usually referred to as the PNC-HF equations [46]. The linearization of these equations with respect to the parameter μ would make them inhomogeneous. Since in our calculations we do not perform such a linearization, the equations remain homogeneous. In this case the PNC amplitude can be calculated using the equation

$$E_{\rm PNC} = \frac{\partial}{\partial \mu} [\langle \Psi^f(\mu) | D_z | \Psi^i(\mu) \rangle]_{\mu=0}, \tag{63}$$

where $\mathbf{D} = \Sigma_i e \mathbf{r}_i$ is the dipole moment operator and Ψ^i and Ψ^f are the many-electron wave functions of the initial and final states, respectively. They obey the equations

$$H(\mu)\Psi^i(\mu) = E_i(\mu)\Psi^i(\mu), \quad H(\mu)\Psi^f(\mu) = E_f(\mu)\Psi^f(\mu). \tag{64}$$

The many-electron wave functions Ψ^i and Ψ^f are represented by a large number of the configuration state functions (CSFs):

$$\Psi^{JM}(\mu) = \sum_\alpha C_\alpha(\mu) \Phi_\alpha^{JM}(\mu). \tag{65}$$

The CSFs Φ_α^{JM} are linear combinations of the Slater determinants, which are constructed from the one-electron wave functions $u_n(\mu)$. Expansion (65) contains the CFSs of different parity, since the weak interaction is included in the Hamiltonian $H(\mu)$.

The one-electron functions $u_n(\mu)$ are obtained as eigenfunctions of the Dirac-Fock operator in the external field:

$$h_u(\mu) u_n(\mu) = \varepsilon_n(\mu) u_n(\mu), \quad h_u(\mu) = h_{\rm DF}(\mu) + \mu H_W. \tag{66}$$

It should be noted that the Dirac-Fock operator $h_{\rm DF}(\mu)$ depends on the parameter μ, since the one-particle density matrix is constructed from occupied orbitals $u_n(\mu)$. We can also consider the set of one-electron wave functions $u_n^0(\mu)$ defined by equations

$$h_u^0(\mu) u_n^0(\mu) = \varepsilon_n^0(\mu) u_n^0(\mu), \quad h_u^0(\mu) = h_{\rm DF}(0) + \mu H_W, \tag{67}$$

where $h_{\rm DF}(0)$ is the standard Dirac-Fock operator without the external field.

The PNC amplitude can be calculated in the Hartree-Fock approximation by using only one CSF in expansion (65). Using Eq. (63) and the wave functions $u_n^0(\mu)$, one obtains the so-called Dirac-Fock value of the PNC amplitude. If the set of $u_n(\mu)$ is used, the method, in principle, is equivalent to the PNC-HF method, which was used by different authors [47–49].

In the large-scale configuration-interaction (CI) method the set of the CSFs for given quantum numbers JM is generated including all single, double, and the most significant part of triple excitations in the positive spectrum of the one-electron states $u_n(\mu)$. In what follows, this method of evaluation of the PNC amplitude will be referred to as the PNC-CI method.

To obtain the set of the one-electron functions $u_n(\mu)$ and $u_n^0(\mu)$, we solve Eqs. (66) and (67) using the finite basis approximation,

$$u_n(\mu) = \sum_a c_a^n(\mu) \varphi_a \tag{68}$$

with the basis functions φ_a given in the central field approximation:

$$\varphi_a(\mathbf{r}) = \frac{i^{l_a}}{r} \begin{pmatrix} P_a(r) & \chi_{\kappa_a m_a}(\mathbf{n}) \\ iQ_a(r) & \chi_{-\kappa_a m_a}(\mathbf{n}) \end{pmatrix}. \tag{69}$$

The representation (69) differs from the standard one by the factor i^l. This factor is introduced to make the one-electron matrix elements of the PNC Hamiltonian be real:

$$\langle a | \gamma^5 \rho_N | b \rangle = -(-1)^{(l_b - l_a + 1)/2} \delta_{\kappa_a, -\kappa_b} \delta_{m_a, m_b} \times \int_0^\infty dr\, \rho_N [P_a Q_b - Q_a P_b], \tag{70}$$

where $l_a + l_b + 1$ is even. With this one-electron basis, the

TABLE VI. The E_{PNC} amplitude, in units of $i\times10^{-11}(-Q_W)/N$ a.u., calculated by different methods without the Breit correction.

		R_N (fm)	DF	PNC-HF	PNC-CI	Others
^{85}Rb	$5s\rightarrow6s$	4.246	−0.110	−0.138	−0.134	−0.135[a]
^{133}Cs	$6s\rightarrow7s$	4.837	−0.741	−0.926	−0.904	−0.906[b]
						−0.908[c]
^{223}Fr	$7s\rightarrow8s$	5.640	−13.72	−16.63	−15.72	−15.56[d]
						−15.8[e]
		5.658 [52]	−13.69	−16.60	−15.69	
^{210}Fr	$7s\rightarrow8s$	5.539	−12.51	−15.17	−14.34	
		5.545 [52]	−12.51	−15.16	−14.34	

[a]PNC−HF+MBPT [49].
[b]MBPT [7].
[c]Correlation potential plus MBPT [13].
[d]MBPT [26].
[e]Correlation Potential+MBPT [25]. The original value, −15.9 [25], is rescaled to R_N=5.640 according to the corresponding analysis presented in Ref. [26].

large-scale PNC-CI matrix is also real and Hermitian.

For the occupied atomic shells, the large P_a and small Q_a components of the radial wave functions are obtained by solving the standard radial DF equations. For the vacant shells the Dirac-Fock-Sturm equations are used. For details of the Dirac-Fock-Sturm method we refer to Refs. [45,50]. The basis set containing the radial functions up to 17*s*, 16*p*, 12*d*, 7*f*, 5*g*, and 2*h* states was used in the calculations.

In the calculations of the one-electron PNC matrix elements (70) we used the Fermi nuclear distribution

$$\rho_N(r)=\frac{\rho_0}{1+e^{4\ln 3(r-c)/t}}, \tag{71}$$

where t=2.3 fm. The parameters c and ρ_0 were determined to reproduce the value of the nuclear mean-square radius $R_N=\langle r^2\rangle^{1/2}$ and the normalization condition for $\rho_N(r)$.

In Table VI we present the results of our calculations of the PNC amplitude for Rb, Cs, and Fr. The results obtained by the DF method are given in the third column. Our DF value for the 6*s*-7*s* PNC transition in Cs, −0.741, is in a good agreement with the values −0.742 [10] and −0.739 [11], which were obtained by the direct summation over the intermediate states. For the 7*s*-8*s* PNC transition in Fr our DF value, −13.72, is also in a good agreement with the −13.56 result obtained in Ref. [26]. Our PNC-HF values, −0.138 for Rb and −0.926 for Cs, can be compared with the values −0.139 and −0.927, respectively, obtained by a similar method in Ref. [49]. In the fifth column of the table, we present our PNC-CI values, which include the core-polarization correlation effects. The uncertainty of these values is estimated to be on the 1% level. For comparison, the most accurate results by other authors are listed in the sixth column of the table. In the second column we give the values of the nuclear-mean-square radius R_N, which were used in our calculations. They were obtained by the formula $R_N=0.836A^{1/3}+0.570$ [51]. In the case of Fr, the corresponding results with R_N taken from Ref. [52] are also presented.

To calculate the contribution of the frequency-independent Breit interaction (BI) to the PNC amplitude, we included the magnetic $V_{\mathrm{G}}^{\mathrm{int}}$ and retardation $V_{\mathrm{R}}^{\mathrm{int}}$ terms in all stages of the calculations. As the first step, the BI was included in the radial Dirac-Fock equations. We will refer this approach to as the Dirac-Fock-Breit (DFB) method. On the second stage, the BI was added to the Dirac-Fock-Sturm equations and to the Dirac-Fock Hamiltonian $h_u(\mu)$ in the external field (66). This method of calculation of the PNC amplitude will be called the PNC-HFB method. Finally, we added the BI to the many-electron Hamiltonian $H(\mu)$ in the external field and performed the large scale CI calculation. This approach will be called the PNC-CIB method. To estimate the role of the retardation part of the Breit intaraction, we repeated all the calculations including only the magnetic (Gaunt) part $V_{\mathrm{G}}^{\mathrm{int}}$ of the BI and then took the difference with the PNC amplitude, which includes the total BI.

In Table VII we present the magnetic Breit $\delta E_{\mathrm{PNC}}^{\mathrm{M}}$ and retardation Breit $\delta E_{\mathrm{PNC}}^{\mathrm{R}}$ contibutions to the 6*s*-7*s* PNC amplitude in ^{133}Cs and to the 7*s*-8*s* PNC amplitude in ^{223}Fr, obtained by different methods. The comparison of the total Breit correction to the PNC amplitude with the most accurate results by other authors are presented in Table VIII. Finally, in the case of francium, our PNC-CIB value amounts to −15.58(16) [R_N=5.640 fm] and −15.55(16) [R_N=5.658 fm]

TABLE VII. The Breit magnetic ($\delta E_{\mathrm{PNC}}^{\mathrm{M}}$), the Breit retardation ($\delta E_{\mathrm{PNC}}^{\mathrm{R}}$), and the total Breit ($\delta E_{\mathrm{PNC}}^{\mathrm{B}}$) correction to the PNC amplitude, in units of $i\times10^{-11}(-Q_W)/N$ a.u.

		DFB	PNC-HFB	PNC-CIB
^{133}Cs	$\delta E_{\mathrm{PNC}}^{\mathrm{M}}$	0.0028	0.0023	0.0049
	$\delta E_{\mathrm{PNC}}^{\mathrm{R}}$	−0.0006	−0.0005	−0.0004
	$\delta E_{\mathrm{PNC}}^{\mathrm{B}}$	0.0022	0.0018	0.0045
^{223}Fr	$\delta E_{\mathrm{PNC}}^{\mathrm{M}}$	0.080	0.082	0.165
	$\delta E_{\mathrm{PNC}}^{\mathrm{R}}$	−0.016	−0.017	−0.022
	$\delta E_{\mathrm{PNC}}^{\mathrm{B}}$	0.064	0.065	0.143

TABLE VIII. Comparison of the total Breit correction to the PNC amplitude, in units of $i\times10^{-11}(-Q_W)/N$ a.u., with the most accurate results by other authors.

^{133}Cs		^{223}Fr	
This work	0.0045	This work	0.14
Kozlov *et al.* [10]	0.004	Safronova and Johnson [26]	0.15
Dzuba *et al.* [13]	0.0055	Derevianko [53]	0.18
Derevianko [12]	0.0054		

for ^{223}Fr, and −14.21(14) for ^{210}Fr. They are in a fair agreement with the most accurate previous results [26], −15.41(17) [R_N=5.640 fm] for ^{223}Fr and −14.02(15) for ^{210}Fr.

IV. TOTAL PNC AMPLITUDES

To get the total $6s$-$7s$ PNC transition amplitude in ^{133}Cs, we combine the most accurate value that includes the correlation and Breit effects [13], −0.902(5), with the −0.27(3)% binding QED correction, the −0.19(6)% neutron skin correction [12], the −0.08% correction due to the renormalization of Q_W from the atomic momentum transfer $q\sim30$ MeV down to $q=0$ [19], and the 0.04% contribution from the electron-electron weak interaction [19,54]. The analysis of accuracy of the atomic structure PNC calculations [6,8,10,13] is based on calculations of the hyperfine splitting, decay rates, and energy levels. As it was argued in Ref. [19], QED corrections to these quantities can be neglected on the 0.5% accuracy level. Using the experimental value for $E_{\rm PNC}/\beta$ [4] and an average value from two most accurate measurements of the vector transition polarizabilty, $\beta=26.99(5)a_{\rm B}^3$ [5,13,55,56], we obtain for the weak charge of ^{133}Cs:

$$Q_W=-72.65(29)_{\rm exp}(36)_{\rm th}. \tag{72}$$

This value deviates from the SM prediction of −73.19(13) [57] by 1.1σ.

In case of francium, combining our PNC-CIB values, −15.55(16) for ^{223}Fr and −14.21(14) for ^{210}Fr, with the −0.28(5)% QED correction and the −0.08% correction due to the renormalization of Q_W from the atomic momentum transfer $q\sim30$ MeV down to $q=0$ [19], we obtain −15.49(16) for ^{223}Fr and −14.16(14) for ^{210}Fr.

In summary, we have calculated the QED correction to the PNC transition amplitude in Cs and Fr. In addition, we have performed an independent high-precision calculation of the correlation and Breit interaction effects on the PNC amplitude in Fr. We have derived the weak charge of ^{133}Cs, which deviates by 1.1σ from the SM prediction. Further improvement of atomic tests of the standard model can be achieved, from the theoretical side, by more accurate calculations of the electron-correlation effects and, from the experimental side, by more precise measurements of the PNC amplitude in cesium or other atomic systems, particularly, in francium [24,58].

ACKNOWLEDGMENTS

Valuable discussions with K.T. Cheng, V.A. Dzuba, V.V. Flambaum, M.Y. Kuchiev, M.S. Safronova, and O.P. Sushkov are gratefully acknowledged. This work was supported by EU (Grant No. HPRI-CT-2001-50034), RFBR (Grant No. 04-02-17574), NATO (Grant No. PST.CLG.979624), and DFG. G.P. acknowledges financial support by the BMBF, DFG, and GSI.

APPENDIX A: ZERO-POTENTIAL PNC VERTEX CONTRIBUTION

The zero-potential PNC vertex contribution is defined as

$$\langle b|\Lambda_W|a\rangle\equiv\int\frac{d\mathbf{p}}{(2\pi)^3}\int\frac{d\mathbf{p}'}{(2\pi)^3}\bar{\psi}_b(\mathbf{p}')\Gamma^0_W(p',p)\times V_W(|\mathbf{p}'-\mathbf{p}|)\psi_a(\mathbf{p}), \tag{A1}$$

where $p=(\varepsilon,\mathbf{p})$ and $p'=(\varepsilon',\mathbf{p}')$ are four vectors,

$$\Gamma^0_W(p',p)=-4\pi i\alpha\int\frac{d^4k}{(2\pi)^4}\gamma_\sigma\frac{\not p'-\not k+m}{(p'-k)^2-m^2}\gamma^0\gamma^5\times\frac{\not p-\not k+m}{(p-k)^2-m^2}\gamma^\sigma\frac{1}{k^2}, \tag{A2}$$

$$V_W(q)\equiv\eta\int d\mathbf{r}\,\rho_N(r)\exp(i\mathbf{q}\cdot\mathbf{r})=\eta\frac{4\pi}{q}\int_0^\infty dr\,r\rho_N(r)\sin(qr), \tag{A3}$$

$q=|\mathbf{q}|$, $r=|\mathbf{r}|$, and $\eta=-(G_F/\sqrt{8})Q_W$. In Eq. (A1), it is implicit that $\varepsilon=\varepsilon_a$ and $\varepsilon'=\varepsilon_b$. One can easily express $\Gamma^0_W(p',p)$ in terms of the standard vertex function $\Gamma^0(p',p)$:

$$\Gamma^0_W(p',p)=\Gamma^0(p',p)\gamma^5-\frac{\alpha}{\pi}[2\varepsilon' m(C_0+C_{11})+2\varepsilon mC_{12}-m^2\gamma^0C_0]\gamma^5, \tag{A4}$$

where the coefficients C_0, C_{11}, and C_{12} are defined as in Ref. [30]. After the isolation of the ultraviolet divergences in $\Gamma^0(p',p)$, the finite part is given by

$$\Gamma^0_{W,R}(p',p)=\frac{\alpha}{4\pi}[(A+4m^2C_0)\gamma_0+\not p'(B_1\varepsilon'+B_2\varepsilon)+\not p(C_1\varepsilon'+C_2\varepsilon)+D\not p'\gamma_0\not p+H_1\varepsilon'+H_2\varepsilon-8\varepsilon' m(C_0+C_{11})-8\varepsilon mC_{12}]\gamma^5, \tag{A5}$$

where all the coefficients are defined as in Ref. [30]. Integrating over the angles in Eq. (A1), one can obtain

$$\langle b|\Lambda_{W,R}|a\rangle=-\frac{\alpha}{2(2\pi)^6}i^{l_b-l_a}\delta_{\kappa_b,-\kappa_a}\delta_{m_b,m_a}\int_0^\infty dp\int_0^\infty dp'p^2p'^2\times\int_{-1}^1 d\xi[V_W(q)Q_1(p',p,\xi)P_{l_b}(\xi)+V_W(q)Q_2(p',p,\xi)P_{l_a}(\xi)], \tag{A6}$$

where $P_l(\xi)$ is a Legendre polynomial, $\kappa=(-1)^{j+l+1/2}(j+1/2)$,

$$Q_1 = [A + 4m^2C_0 + \varepsilon'(B_1\varepsilon' + B_2\varepsilon) + \varepsilon(C_1\varepsilon' + C_2\varepsilon) + D\varepsilon'\varepsilon + H_1\varepsilon' + H_2\varepsilon - 8\varepsilon' m(C_0 + C_{11}) - 8\varepsilon m C_{12}]\tilde{g}_b(p')\tilde{f}_a(p) + [p'(B_1\varepsilon' + B_2\varepsilon) + Dp'\varepsilon]\tilde{f}_b(p')\tilde{f}_a(p) + [p(C_1\varepsilon' + C_2\varepsilon) + Dp\varepsilon']\tilde{g}_b(p')\tilde{g}_a(p) + Dp'p\tilde{f}_b(p')\tilde{g}_a(p), \quad \text{(A7)}$$

$$Q_2 = [A + 4m^2C_0 + \varepsilon'(B_1\varepsilon' + B_2\varepsilon) + \varepsilon(C_1\varepsilon' + C_2\varepsilon) + D\varepsilon'\varepsilon - H_1\varepsilon' - H_2\varepsilon + 8\varepsilon' m(C_0 + C_{11}) + 8\varepsilon m C_{12}]\tilde{f}_b(p')\tilde{g}_a(p) + [p'(B_1\varepsilon' + B_2\varepsilon) + Dp'\varepsilon]\tilde{g}_b(p')\tilde{g}_a(p) + [p(C_1\varepsilon' + C_2\varepsilon) + Dp\varepsilon']\tilde{f}_b(p')\tilde{f}_a(p) + Dp'p\tilde{g}_b(p')\tilde{f}_a(p), \quad \text{(A8)}$$

$\tilde{g}(p)$ and $\tilde{f}(p)$ are the radial components of the Dirac wave function in the momentum representation, defined as in Ref. [30].

[1] I. B. Khriplovich, *Parity Nonconservation in Atomic Phenomena* (Gordon and Breach, London, 1991).
[2] I. B. Khriplovich, Phys. Scr., T **112**, 52 (2004).
[3] M. A. Bouchiat and C. Bouchiat, J. Phys. (Paris) **35**, 899 (1974); **36**, 493 (1974).
[4] C. S. Wood, S. C. Bennett, D. Cho, B. P. Masterson, J. L. Roberts, C. E. Tanner, and C. E. Wieman, Science **275**, 1759 (1997).
[5] S. C. Bennett and C. E. Wieman, Phys. Rev. Lett. **82**, 2484 (1999); **83**, 889 (1999).
[6] V. A. Dzuba, V. V. Flambaum, and O. P. Sushkov, Phys. Lett. A **141**, 147 (1989).
[7] S. A. Blundell, W. R. Johnson, and J. Sapirstein, Phys. Rev. Lett. **65**, 1411 (1990).
[8] S. A. Blundell, J. Sapirstein, and W. R. Johnson, Phys. Rev. D **45**, 1602 (1992).
[9] A. Derevianko, Phys. Rev. Lett. **85**, 1618 (2000).
[10] M. G. Kozlov, S. G. Porsev, and I. I. Tupitsyn, Phys. Rev. Lett. **86**, 3260 (2001).
[11] V. A. Dzuba, C. Harabati, W. R. Johnson, and M. S. Safronova, Phys. Rev. A **63**, 044103 (2001).
[12] A. Derevianko, Phys. Rev. A **65**, 012106 (2001).
[13] V. A. Dzuba, V. V. Flambaum, and J. S. M. Ginges, Phys. Rev. D **66**, 076013 (2002).
[14] O. P. Sushkov, Phys. Rev. A **63**, 042504 (2001).
[15] W. R. Johnson, I. Bednyakov, and G. Soff, Phys. Rev. Lett. **87**, 233001 (2001).
[16] W. J. Marciano and A. Sirlin, Phys. Rev. D **27**, 552 (1983).
[17] B. W. Lynn and P. G. H. Sandars, J. Phys. B **27**, 1469 (1994).
[18] M. Y. Kuchiev, J. Phys. B **35**, L503 (2002); M. Y. Kuchiev and V. V. Flambaum, Phys. Rev. Lett. **89**, 283002 (2002).
[19] A. I. Milstein, O. P. Sushkov, and I. S. Terekhov, Phys. Rev. Lett. **89**, 283003 (2002); Phys. Rev. A **67**, 062103 (2003).
[20] M. Y. Kuchiev and V. V. Flambaum, J. Phys. B **36**, R191 (2003).
[21] J. Sapirstein, K. Pachucki, A. Veitia, and K. T. Cheng, Phys. Rev. A **67**, 052110 (2003).
[22] V. M. Shabaev, K. Pachucki, I. I. Tupitsyn, and V. A. Yerokhin, Phys. Rev. Lett. **94**, 213002 (2005).
[23] V. V. Flambaum and J. S. M. Ginges, e-print physics/0507067.
[24] J. A. Behr, S. B. Cahn, S. B. Dutta, A. Gorlitz, A. Ghosh, G. Gwinner, L. A. Orozco, G. D. Sprouse, and F. Xu, Hyperfine Interact. **81**, 197 (1993) [CAS]; L. A. Orozco, J. E. Simsarian, G. D. Sprouse, and W. Z. Zhao, in *First Latin American Symposium on High Energy Physics and VII Mexican School of Particles and Fields*, edited by J. C. D'Olivo, M. Klan-Kreisler, and H. Mndez, AIP Conf. Proc. No. 400 (AIP, New York, 1997), p. 107.
[25] V. A. Dzuba, V. V. Flambaum, and O. P. Sushkov, Phys. Rev. A **51**, 3454 (1995).
[26] M. S. Safronova and W. R. Johnson, Phys. Rev. A **62**, 022112 (2000).
[27] V. M. Shabaev, Teor. Mat. Fiz. **82**, 83 (1990) [Theor. Math. Phys. **82**, 57 (1990)]; Izv. Vyssh. Uchebn. Zaved. Fiz. **33**, 43 (1990) [Sov. Phys. JETP **33**, 660 (1990)]; Phys. Rev. A **50**, 4521 (1994).
[28] V. M. Shabaev, Phys. Rep. **356**, 119 (2002).
[29] N. J. Snyderman, Ann. Phys. **211**, 43 (1991).
[30] V. A. Yerokhin and V. M. Shabaev, Phys. Rev. A **60**, 800 (1999); V. A. Yerokhin, A. N. Artemyev, T. Beier, G. Plunien, V. M. Shabaev, and G. Soff, *ibid.* **60**, 3522 (1999).
[31] J. Sapirstein and K. T. Cheng, Phys. Rev. A **66**, 042501 (2002).
[32] A. G. Fainshtein, N. L. Manakov, and A. A. Nekipelov, J. Phys. B **24**, 559 (1991).
[33] V. F. Bratzev, G. B. Deyneka, and I. I. Tupitsyn, Izv. Akad. Nauk SSSR, Ser. Fiz. **41**, 2655 (1977) [Bull. Acad. Sci. USSR, Phys. Ser. (Engl. Transl.) **41**, 173 (1977)].
[34] C. E. Moore, *Atomic Energy Levels*, Natl. Bur. Stand. Ref. Data Ser., Natl. Bur. Stand. (U.S.) Circ. No. 35 (U.S. GPO, Washington, D.C., 1971), Vol. I-III.
[35] J. Bauche H. T. Duong, P. Juncar, S. Liberman, J. Pinard, A. Coc, C. Thibault, F. Touchard, J. Lerme, J. L. Vialle, S. Buttgenbach, A. C. Mueller, and A. Pesnelle, **19**, L593 (1986).
[36] H. T. Duong, P. Juncar, S. Liberman, A. C. Mueller, R. Neugart, E. W. Otten, B. Peuse, J. Pinard, H. H. Stroke, C. Thibault, F. Touchard, J. L. Vialle, K. Wendt, and the ISOLDE Collaboration, Europhys. Lett. **3**, 175 (1987).
[37] S. V. Andreev, V. S. Letokhov, and V. I. Mishin, Phys. Rev. Lett. **59**, 1274 (1987); S. V. Andreev, V. I. Mishin, and V. S. Letokhov, J. Opt. Soc. Am. B **5**, 2190 (1988).
[38] E. Arnold, W. Borchers, H. T. Duong, P. Juncar, J. Lerme, P. Lievens, W. Neu, R. Neugart, M. Pellarin, J. Pinard, J. L. Vialle, K. Wendt, and the ISOLDE Collaboration, J. Phys. B **23**, 3511 (1990).
[39] J. E. Simsarian, W. Shi, L. A. Orozco, G. D. Sprouse, and W. Z. Zhao, Opt. Lett. **21**, 1939 (1996).
[40] J. E. Simsarian, W. Z. Zhao, L. A. Orozco, and G. D. Sprouse, Phys. Rev. A **59**, 195 (1999).
[41] J. M. Grossman, R. P. Fliller, III, T. E. Mehlstäubler, L. A.

Orozco, M. R. Pearson, G. D. Sprouse, and W. Z. Zhao, Phys. Rev. A **62**, 052507 (2000).
[42] V. M. Shabaev, I. I. Tupitsyn, V. A. Yerokhin, G. Plunien, and G. Soff, Phys. Rev. Lett. **93**, 130405 (2004).
[43] J. Sucher, Phys. Rev. A **22**, 348 (1980).
[44] M. H. Mittleman, Phys. Rev. A **24**, 1167 (1981).
[45] D. A. Glazov, V. M. Shabaev, I. I. Tupitsyn, A. V. Volotka, V. A. Yerokhin, G. Plunien, and G. Soff, Phys. Rev. A **70**, 062104 (2004).
[46] P. G. H. Sandars, J. Phys. B **10**, 2983 (1977).
[47] C. E. Loving and P. G. H. Sandars, J. Phys. B **8**, L336 (1975).
[48] W. R. Johnson, D. S. Guo, M. Idrees, and J. Sapirstein, Phys. Rev. A **32**, 2093 (1985).
[49] W. R. Johnson, D. S. Guo, M. Idrees, and J. Sapirstein, Phys. Rev. A **34**, 1043 (1986).
[50] I. I. Tupitsyn, V. M. Shabaev, J. R. Crespo López-Urrutia, I. Draganić, R. S. Orts, and J. Ullrich, Phys. Rev. A **68**, 022511 (2003).
[51] W. R. Johnson and G. Soff, At. Data Nucl. Data Tables **33**, 405 (1985).
[52] I. Angeli, At. Data Nucl. Data Tables **87**, 185 (2004).
[53] A. Derevianko, e-print, physics/0001046 (2000).
[54] O. P. Sushkov and V. V. Flambaum, Yad. Fiz. **27**, 1307 (1978).
[55] D. Cho, C. S. Wood, S. C. Bennett, J. L. Roberts, and C. E. Wieman, Phys. Rev. A **55**, 1007 (1997).
[56] A. A. Vasilyev, I. M. Savukov, M. S. Safronova, and H. G. Berry, Phys. Rev. A **66**, 020101(R) (2002).
[57] J. L. Rosner, Phys. Rev. D **65**, 073026 (2002).
[58] R. Calabrese (private communication).